

# Preparation of a Tubular Palladium Membrane by Photocatalytic Deposition

Hong Qian, Lixiong Zhang and Nanping Xu<sup>†</sup>

Membrane Science & Technology Research Center, Nanjing University of Technology, Nanjing 210009, P. R. China

(Received 3 May 2002 • accepted 5 September 2002)

**Abstract**—A novel photocatalytic deposition method for the preparation of a thin tubular palladium membrane is presented in this paper. The membrane is prepared on a porous asymmetric  $\text{TiO}_2$  support by photocatalytic reaction of palladium ion, followed by electroless plating. Gas permeation results show that the membrane exhibits increased hydrogen permeance with the increase of temperature. The hydrogen permeance and selectivity to nitrogen at 773 K are about  $1.43 \times 10^{-6} \text{ mol m}^{-2} \text{ s}^{-1} \text{ Pa}^{-1}$  and 17, respectively, when the pressure in the feed side is 0.1 MPa. The activation energy of hydrogen permeation is 11.06 kJ/mol at the temperature range of 573-773 K.

Key words: Palladium Membrane,  $\text{TiO}_2$  Membrane, Photocatalytic Deposition, Electroless Plating, Hydrogen Separation

## INTRODUCTION

Hydrogen is an environment-friendly and renewable fuel and a very important chemical material. Palladium-based membranes have been studied extensively due to their extremely high hydrogen permselectivity and the applications to membrane reactors [Nam et al., 2000]. On the other hand, the membrane process can make more efficient use of energy than other separation such as adsorption. In recent years, research on palladium-based membranes has been focused on composite palladium membranes because pure palladium possesses disadvantages such as high cost, low hydrogen permeance and low stability, which are the hurdles to the commercialization of palladium membranes [Li et al., 1994]. Composite palladium membranes, which consist of a thin Pd film supported on a porous ceramic substrate, have been investigated as a means of improving hydrogen permeance and lowering the cost of the membranes. Various kinds of methods have been reported to synthesize the composite membranes, including chemical vapor deposition (CVD), physical vapor deposition (PVD), electroplating, and electroless plating, spray pyrolysis, etc. [Jayaraman et al., 1995; Aoki et al., 1996; Xomeritakis and Lin, 1998; Nam et al., 1999; Li et al., 2000]. Each method has its own disadvantages. For example, CVD requires too high purity of constituents and strict process conditions; PVD has difficulty in forming defect-free membranes, and so on. Electroless plating is an attractive technique for producing such membranes, due to the possibility of uniform deposition on complex shapes and relatively simple equipment. However, it also suffers from difficulties in controlling the film thickness and complicated pretreatment.

Recently, a novel technique called photocatalytic deposition was invented in our laboratory [Wu et al., 2000a, b]. The mechanism is a photocatalytic reaction between the surface of the  $\text{TiO}_2$  semiconductor and the Pd(II) solution. We applied it in preparing palladium membranes supported on disk-shaped  $\text{TiO}_2$  membranes. The resulting membranes have thickness of 300-400 nm, hydrogen permeance of  $6.0 \times 10^{-6} \text{ mol m}^{-2} \text{ s}^{-1} \text{ Pa}^{-1}$ , and  $\text{H}_2 : \text{N}_2$  permselectivity of 1,140 at 773 K [Wu et al., 2000]. Apparently, this novel tech-

nique omits the conventional labor-consuming pretreatment in the preparation of palladium membrane via electroless plating, which always introduces foreign elements and results in a decrease of hydrogen selectivity. In this paper, a palladium membrane supported on a porous  $\text{TiO}_2$  ceramic tube is prepared by using this technique. Factors affecting the photocatalytic deposition are investigated including light intensity, initial reactant concentration, reaction temperature, and reaction time. The structure and performance of the palladium membrane are also examined.

## EXPERIMENTAL

### 1. Preparation of the Palladium Membrane

The  $\text{TiO}_2$  (anatase) tubular membrane on an  $\alpha\text{-Al}_2\text{O}_3$  support (O.D.

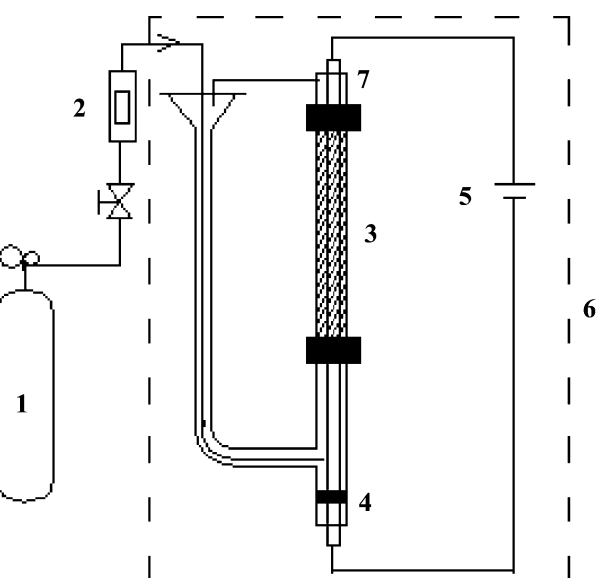


**Fig. 1. Schematic diagram of experimental setup for a photocatalytic deposition.**

1. Gas cylinders	5. Power supply
2. Mass flow controller	6. Thermostat
3. Ceramic tube	7. Light source
4. Seal ring	

<sup>†</sup>To whom correspondence should be addressed.

E-mail: npxu@njuct.edu.cn

10 mm, I.D. 8 mm, Length 110 mm, two ends coated with glaze) is synthesized from colloidal titania sols by dip-coating. The hydrogen and nitrogen permeance of the supported  $\text{TiO}_2$  membrane is  $2.1 \times 10^{-5}$  and  $6.0 \times 10^{-6} \text{ mol m}^{-2} \text{ s}^{-1} \text{ Pa}^{-1}$ , respectively.

Photocatalytic deposition is carried out on a defect-free  $\text{TiO}_2$  membrane in a setup shown in Fig. 1. The light source with outer diameter of 6 mm is specially made to insert into the membrane tube to make sure of uniform distribution of the ultraviolet light. The whole setup is put in a thermostat to guarantee a uniform reaction temperature. The reagents used are  $\text{PdCl}_2$ ,  $\text{CH}_3\text{OH}$ ,  $\text{HCl}$  and double-distilled water.

During the photocatalytic deposition process,  $\text{PdCl}_2$  solution is added from the left funnel and contacts the inner surface of the tubular  $\text{TiO}_2$  membrane via a U shape pipe. High-pure  $\text{N}_2$  is introduced all over the process to drive off the dissolved oxygen in the solution. After a certain reaction time, the membrane is uninstalled from the setup, washed with double-distilled water and dried in  $\text{N}_2$  atmosphere for 14 h.

In order to improve  $\text{H}_2/\text{N}_2$  permselectivity of the palladium membrane after photocatalytic deposition, electroless plating is used to heal the palladium membrane. The composition of the electroless plating bath and the electroless plating conditions are listed in Table 1. After 40 minutes, the membrane is taken out, washed and then dried in  $\text{N}_2$  atmosphere overnight.

## 2. Characterization of the Membrane

The morphology, the purity, surface element analysis and the valence state of the surface element of the palladium membrane are examined by Scanning Electronic Microscopy (SEM, JEOL JSM-

**Table 1. Composition and conditions in the electroless plating**

$\text{PdCl}_2$	3.9 g/L
$\text{Na}_2\text{EDTA}$	350 mL/L
$\text{NH}_4\text{OH}$	50 g/L
$\text{N}_2\text{H}_4$	11 mL/L
PH	11
Temperature	65 °C

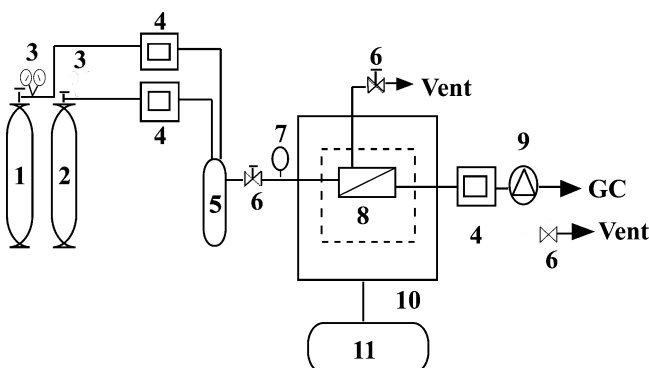


**Fig. 2. Apparatus for gas permeation test through Pd membrane at high temperature.**

1, 2. Gas cylinders	7. Pressure gauge
3. Two-stage regulator	8. Stainless steel permeator
4. Mass flow controller	9. Six-way valve
5. Gas-mixer	10. Pipe furnace
6. Flow control valve	11. Thermostatic regulator

6300), X-ray diffraction (XRD, Rigaku D/MAX-rB,  $\text{Cu K}\alpha$  radiation), energy-dispersive X-ray spectroscopy (EDS, Kevex-Sigma, electron source 15 KV, beams current 100 pA) and x-ray photo-electronic spectrum (XPS, VG Scientific Ltd.), respectively.

## 3. Gas Permeation Measurements

The gas permeation measurement apparatus is shown in Fig. 2. The resulting membrane is placed inside a stainless steel permeator using graphite gasket rings as sealers. Then the permeator is installed in a tubular furnace whose temperature is controlled by a micro-processor temperature controller (Model 708PA). During the course of measurement, gases are supplied from the feed side and the permeation side is maintained at atmospheric pressure. The flow rate through the membrane is measured by a bubble flow meter.

## RESULTS AND DISCUSSION

### 1. Effect of Light Intensity

Light intensity has a significant effect on the photocatalytic deposition, as shown in Fig. 3. It is apparent that  $\text{Pd(II)}$  concentration

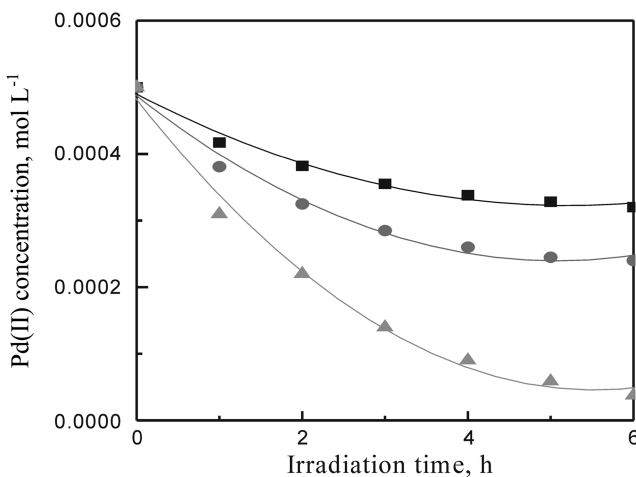


**Fig. 3.  $\text{Pd(II)}$  remaining as a function of irradiation time at various light intensity.**

(■)  $75 \mu\text{w}/\text{cm}^2$ ; (●)  $100 \mu\text{w}/\text{cm}^2$ ; (▲)  $150 \mu\text{w}/\text{cm}^2$

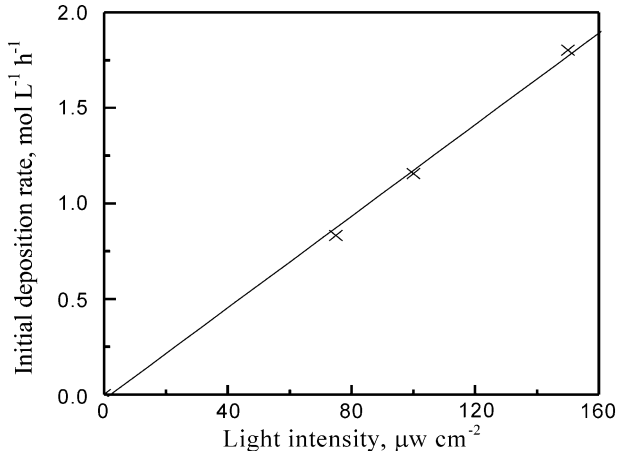


**Fig. 4. Initial deposition rate plotted as a function of light intensity.**

decreases faster when light intensity is increased, which indicates that more Pd(II) is transferred into Pd via photocatalytic reaction. We cannot observe the deposition of Pd in the bulk solution, which means that Pd formed by photocatalytic reaction deposits on the surface of  $\text{TiO}_2$  membrane.

Fig. 4 displays the initial deposition rate as a function of light intensity. Higher light intensity results in higher Pd deposition rate. In order to increase the efficiency of the photocatalytic deposition, higher light intensity is preferred. In this experiment,  $150 \mu\text{m}/\text{cm}^2$  is chosen.

## 2. Effect of Initial Pd(II) Concentration

Photocatalytic deposition is mainly concentrated on the surface interface, which is completed via diffusion, adsorption, surface reaction and desorption. As an immobilized system, the total reaction rate of heterogeneous photocatalytic reaction is only determined by surface reaction in conditions that reactant adsorption and desorption go really quickly and diffusion can be ignored [Fu et al., 1997]. Then the reaction rate  $r$  can be shown as:

$$r = k\theta_A\theta_{OH} \quad (1)$$

$\theta_{OH}$  is considered to be constant and the adsorption of the product on the surface is negligible; then Eq. (1) can be transformed into Eq. (2) according to the Langmuir relation:

$$\frac{1}{r} = \frac{1}{kK_A} \cdot \frac{1}{C_A} + \frac{1}{k} \quad (2)$$

In order to explore the relationship between the photocatalytic reaction rate and initial Pd(II) concentration, we plot the initial rate inverse vs. various initial concentration inverse in Fig. 5, which suggests that the relationship between the photocatalytic reaction rate and initial Pd(II) concentration fits well with the Langmuir-Hinshelwood mechanism. From experimental data,  $k$  and  $K$  is calculated to be  $0.0953 \text{ mmol L}^{-1} \text{ h}^{-1}$  and  $3.696 \text{ L mmol}^{-1}$ , respectively.

It is also found that the photocatalytic deposition process for different initial Pd(II) concentration accords with the first-order reaction kinetics (see Fig. 6). The first-order kinetics equation for the initial concentration of  $0.0005 \text{ mol/L}$  is:

$$\ln(C_0/C) = 0.05871 + 0.42014t \quad (3)$$

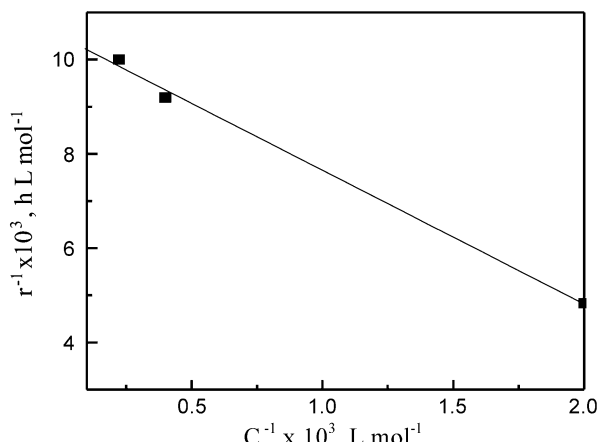


Fig. 5. Langmuir-Hinshelwood plot of Pd(II) photocatalytic reaction.

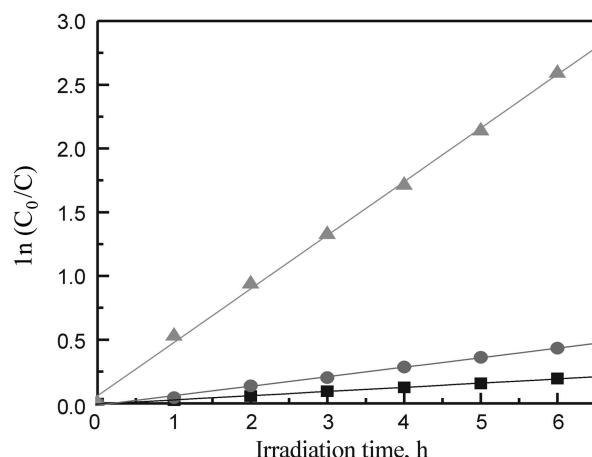


Fig. 6. First-order reaction kinetic for different initial Pd(II) concentration.

(▲)  $0.0005 \text{ mol/L}$ ; (●)  $0.0025 \text{ mol/L}$ ; (■)  $0.0045 \text{ mol/L}$

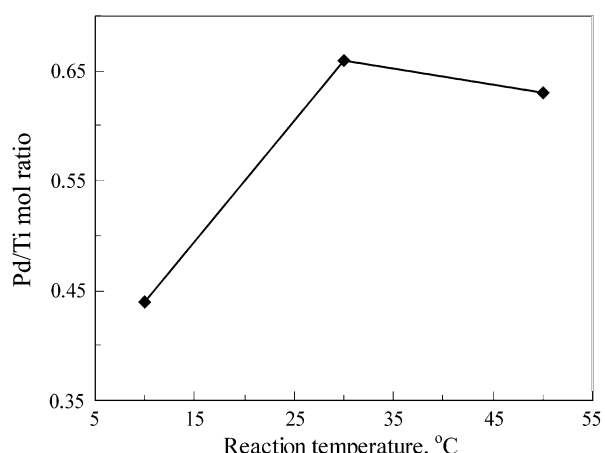


Fig. 7. Temperature dependence of Pd/Ti mol ratio of the membrane after photocatalytic deposition.

The above results suggest that lower initial Pd(II) concentration has a distinct influence on the reaction rate. In this case, we choose initial Pd(II) concentration as  $0.0005 \text{ mol/L}$ .

## 3. Effect of the Reaction Temperature

Fig. 7 shows the temperature dependence of Pd/Ti mol ratio of the membrane after photocatalytic deposition. It is clear that more Pd can be produced at  $303 \text{ K}$  than at  $283 \text{ K}$  and  $323 \text{ K}$ , indicating that  $303 \text{ K}$  is the optimum reaction temperature.

## 4. Effect of the Radiation Time

Radiation time also affects the photocatalytic deposition process. Radiation time dependence of Pd concentration in the solution (Fig. 3) shows that Pd concentration decreases with reaction time, and it almost reaches a steady state value after  $6 \text{ h}$ ; that is to say, the reaction is nearly completed after being radiated for  $6 \text{ h}$ . We can also see from SEM analysis of deposit Pd membranes after various radiation times that Pd particles begin to form on the surface of  $\text{TiO}_2$  after reaction for  $3 \text{ h}$ , but it is not a continuous layer. After reacting for  $6 \text{ h}$ , a uniform Pd settled layer is formed, and when the radiation time is prolonged to  $9 \text{ h}$ , the uniformity of the settled layer is not distinctly improved. Therefore, a radiation time of  $6 \text{ h}$  is pre-

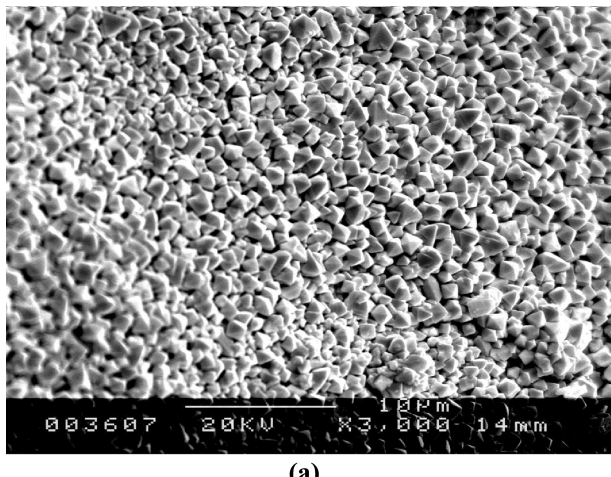
ferred in this study.

From the above results, the photocatalytic deposition conditions are determined: light intensity of  $150 \mu\text{m}/\text{cm}^2$ ; initial Pd(II) concentration of  $0.0005 \text{ mol/L}$ ; reaction temperature of  $303 \text{ K}$ ; radiation time of 6 h. After the photocatalytic reaction finishes, palladium is uniformly dispersed on the top layer of the substrate to form a smooth surface. Gas permeation results show that  $\text{H}_2/\text{N}_2$  permselectivity maintains at 4.7, almost independent of the operating temperature and partial pressure difference.

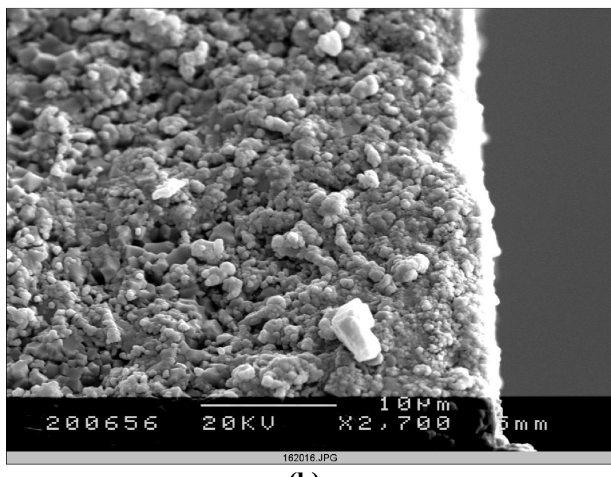
The above permselectivity appears relatively lower for practical applications, which demands a further approach to heal the membrane. Electroless plating is one of the appropriate methods. Unlike the conventional electroless plating technique, no activation step is needed in our case since Pd on the membrane can play the role of catalyst.

### 5. Structure of the Healed Tubular Palladium Membranes

The microstructures of the healed Pd membrane are analyzed by using SEM. As shown in Fig. 8a, a uniform and dense layer with palladium particles regularly arranged has been formed on the substrate. Fig. 8b gives the cross-section SEM image of the healed tubular Pd membrane, indicating a thin continuous layer is deposited on the surface of the support. As determined from Fig. 8b, the thick-



(a)



(b)

**Fig. 8. SEM micrographs of the healed tubular Pd membrane.**  
(a) Surface; (b) Cross-section

ness of the palladium layer is about  $1\text{-}2 \mu\text{m}$ .

The surface elements as well as their valence state are investi-

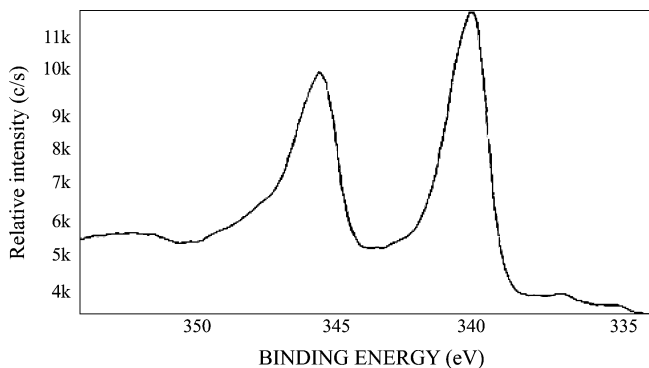


**Fig. 9. XPS results of the healed tubular Pd membrane.**

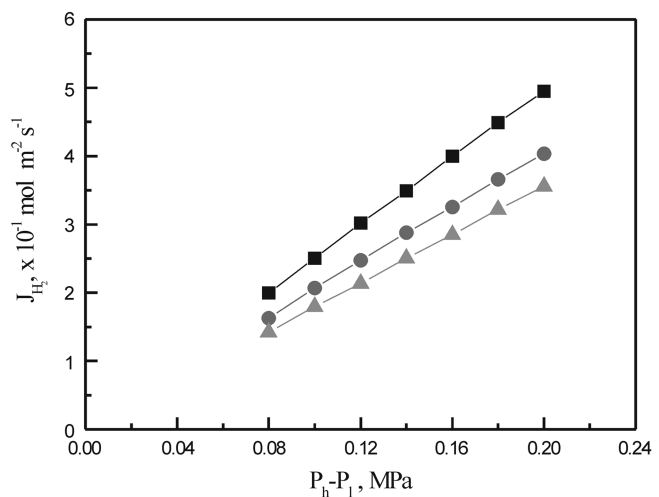


**Fig. 10. Dependence of hydrogen flux on hydrogen partial pressure differences at various temperatures for the healed tubular Pd membrane.**  
(▲)  $T=573 \text{ K}$ ; (●)  $T=673 \text{ K}$ ; (■)  $T=773 \text{ K}$

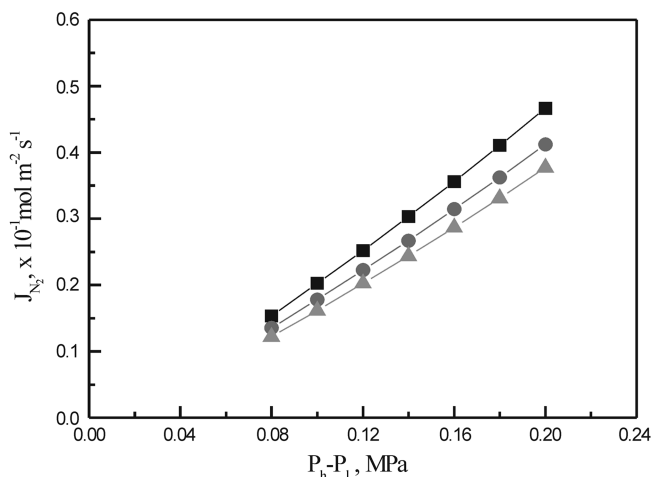


**Fig. 11. Dependence of nitrogen flux on nitrogen partial pressure differences at high temperatures for the healed tubular Pd membrane.**  
(■)  $T=573 \text{ K}$ ; (●)  $T=673 \text{ K}$ ; (▲)  $T=773 \text{ K}$

gated by EDS and XPS analysis, respectively. Fig. 9 shows the XPS results of the healed tubular Pd membrane, which reveals that the main component in the layer is pure palladium.

## 6. Gas Permeation of the Healed Membranes

Fig. 10 and Fig. 11 summarize results of hydrogen/nitrogen permeability experiments performed with the healed membrane mentioned above. It can be seen from the figures that hydrogen flux through the healed membrane increases while nitrogen flux generally decreases with increasing temperatures. The graphs clearly illustrate some important trends in the data. Nitrogen ultimately diffuses through defects in the palladium membrane via Knudsen and surface diffusion, while hydrogen permeating through the dense part of the healed membrane is determined mainly by the solution-diffusion mechanism. The dense part of the healed membrane contributes mostly to hydrogen permeation at high temperatures, which leads to hydrogen increase and nitrogen decrease at elevated temperatures.

Fig. 12 shows the  $H_2/N_2$  permselectivity as a function of temperature and pressure. The permselectivity increases with increasing temperatures and decreasing partial pressure difference. The results accord with Collins report, indicating that with the increase of the pressure, nitrogen flux increases more rapidly than hydrogen flux. A permselectivity of 17 is obtained at 773 K and 0.08 MPa.

According to the Arrhenius theory, activated energy for hydrogen permeation through the membrane can be estimated from the

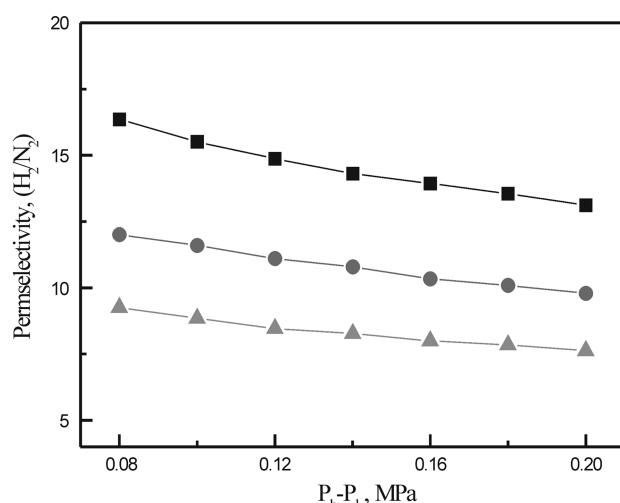


Fig. 12. Permselectivity of hydrogen to nitrogen as a function of hydrogen partial pressure differences at various temperatures.

(▲) T=573 K; (●) T=673 K; (■) T=773 K

Table 2. Summary of the relationship between the metal layer thickness and the activation energy of Pd membrane

Membrane	Preparation method	Thickness ( $\mu\text{m}$ )	$E_a$ (kJ/mol)	Ref
Pd-Ag / $\alpha$ -Al <sub>2</sub> O <sub>3</sub>	MOCVD	0.1-1.5	30	Mccool et al., 1998
Pd/Alumina	Electroless plating	11.4-20	14.45	Collins and Way, 1993
Pd/PG	Electroless plating	13	10.7	Uemiya et al., 1991
Pd/ $\gamma$ -Al <sub>2</sub> O <sub>3</sub>	CVD	0.5-5	13-18	Xomeritakis and Lin, 1998
Pd/ $\alpha$ -Al <sub>2</sub> O <sub>3</sub>	Electroless plating with osmosis	10	12.3	Li et al., 2000
Pd/Al <sub>2</sub> O <sub>3</sub>	CVD	0.5-1	38	Xomeritakis and Lin, 1996
Pd/stainless steel	Electroless plating with osmosis	1	16.4	Mardilovich et al., 1998

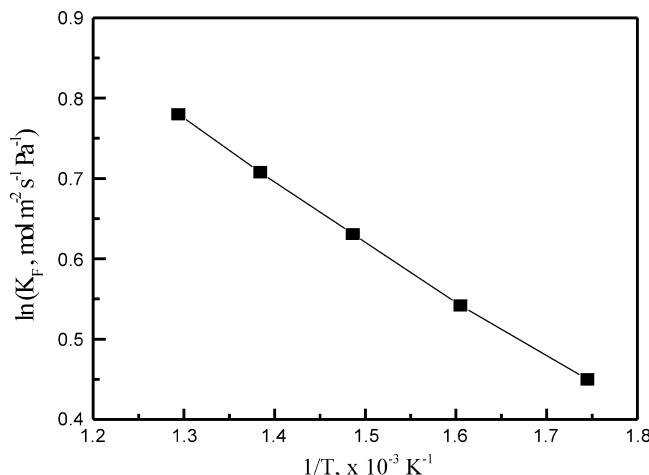


Fig. 13. Arrhenius relation between the hydrogen permeation coefficient and temperature for the healed palladium membrane.

Table 3. Hydrogen permeation through membranes of different material

Membrane	H <sub>2</sub> permeance (mol·l <sup>-1</sup> ·s <sup>-2</sup> ·Pa <sup>-1</sup> )	H <sub>2</sub> /N <sub>2</sub> selectivity
PEI/PES hollow fiber membrane	$1.2 \times 10^{-7}$	162
PEI hollow fiber membrane	$2 \times 10^{-8}$	105
Capillary carbon molecular sieve membrane	$1 \times 10^{-7}$	1000
Silicon-carbon-based membrane	$2.7 \times 10^{-9}$	20
Silica molecular sieve membrane	$2.54 \times 10^{-8}$	90
Silica membrane	$2 \times 10^{-6}$	64
Hydrophobic silica membrane	$1.86 \times 10^{-8}$	8.8
Pd/ceramic	$1 \times 10^{-6}$	10-1000
Pd/Alumina	$7 \times 10^{-7}$	5-24
Pd/glass	$6.52 \times 10^{-7}$	400-1000
Pd/stainless steel	$4.35 \times 10^{-7}$	5-200
Pd/Alumina	$3.83 \times 10^{-7}$	20-130
Pd/TiO <sub>2</sub>	$1.43 \times 10^{-6}$	5-17

permeation data at various temperatures. Fig. 13 shows Arrhenius relation between the hydrogen permeation coefficient and temperature for the healed palladium membrane. The activated energy for hydrogen permeance is 11.06 kJ/mol in a temperature range of 573-773 K, close to the value of 16.4 kJ/mol reported by Mardilovich.

Table 2 summarizes activated energies of palladium membranes prepared by different methods. It shows that all the activated energy of the Pd membrane prepared by electroless plating maintains at about 10 kJ/mol.

Hydrogen permeances through membranes prepared with different materials are shown in Table 3. We can conclude from the table that hydrogen permeance through the membrane is generally on the order of  $10^{-7}$  mol·m<sup>-2</sup>·s<sup>-1</sup>·Pa<sup>-1</sup> or even less, which is a factor of 10 lower than that of the Pd membrane in this work. Higher H<sub>2</sub>/N<sub>2</sub> permselectivity is usually derived from palladium membranes, indicating potential application of this kind of membrane in hydrogen separation in the future.

## CONCLUSIONS

A tubular Pd membrane supported on a crack-free TiO<sub>2</sub> membrane with the thickness of 1-2  $\mu$ m is synthesized via photocatalytic deposition and then healed by electroless plating. The optimal factors for photocatalytic deposition are determined: light intensity of 150  $\mu$ m/cm<sup>2</sup>; initial Pd(II) concentration of 0.0005 mol/L; reaction temperature of 303 K; Radiation time of 6 h. The tubular composite palladium membrane exhibits high hydrogen permeance of  $1.43 \times 10^{-6}$  mol m<sup>-2</sup> s<sup>-1</sup> Pa<sup>-1</sup> and H<sub>2</sub>/N<sub>2</sub> permselectivity of 17. Hydrogen permeance through the membrane increases with increase of temperature, in accordance with the solubility-diffusion law. The activation energy for hydrogen permeance is 11.06 kJ/mol in a temperature range of 573-773 K.

## REFERENCES

Aoki, K., Yokoyama, S., Kusakabe, K. and Morooka, S., "Preparation of Supported Palladium Membrane and Separation of Hydrogen," *Korean J. Chem. Eng.*, **13**, 530 (1996).

Collins, J. P. and Way, J. D., "Preparation and Characterization of a Composite Palladium-ceramic Membrane," *Ind. Eng. Chem. Res.*, **32**(12), 3006 (1993).

Fu, H. X., Lv, G. X. and Li, S. B., "Cr<sup>6+</sup> Photoreduction in the Presence of Organic," *Wuli Huaxue Xuebao*, **13**(2), 106 (1997).

Jayaraman, V., Lin, Y. S. and Pakala, M., "Fabrication of Ultrathin Metallic Membranes on Ceramic Supports by Sputter Deposition," *J. Membr. Sci.*, **99**, 89 (1995).

Li, A., Liang, W. Q. and Hughes, R., "Fabrication of Dense Palladium Composite Membranes for Hydrogen Separation," *Catalysis Today*, **56**, 45 (2000).

Li, A., Xiong, G. and Zheng, L., "Metal Composite Membrane," *Huaxue Jinzhan*, **6**(2), 142 (1994).

Mardilovich, P. P., She, Y. and Ma, Y. H., "Defect-free Palladium Membranes on Porous Stainless Steel Support," *AIChE J.*, **44**(2), 310 (1998).

Mccool, B., Collins, J. P. and Way, J. D., "Sputter Deposition Synthesis and Properties of Ultrathin Metallic Membranes," in S.-I. Nakao (Ed.), *Proc. 5<sup>th</sup> Int. Conf. Iorg. Membranes*, Nagoya, Japan, June, 678 (1998).

Nam, S. E., Lee, S. H. and Lee, K. H., "Preparation of a Palladium Alloy Composite Membrane Supported in a Porous Stainless Steel by Vacuum Electrodeposition," *J. Memb. Sci.*, **153**, 163 (1999).

Nam, S. W., Yoon, S. P. and Ha, H. Y., "Methane Steam Reforming in a Pd-Ru Membrane Reactor," *Korean J. Chem. Eng.*, **17**, 288 (2000).

Uemiya, S., Sato, N., Ando, H., Kude, Y., Matsuda, T. and Kikuchi, E., "Separation of Hydrogen through Palladium Thin Film Supported on a Porous Glass Tube," *J. Memb. Sci.*, **56**, 303 (1991).

Wu, L. Q., Xu, N. P. and Shi, J., "Novel Method for Preparing Palladium Membranes by Photocatalytic Deposition," *AIChE J.*, **46**(5), 1075 (2000).

Wu, L. Q., Xu, N. P. and Shi, J., "Preparation of a Palladium Composite Membrane by an Improved Electroless Plating Technique," *Ind. Eng. Chem. Res.*, **39**, 342 (2000).

Xomeritakis, G. and Lin, Y. S., "CVD Synthesis and Gas Permeation Properties of Thin Palladium/Alumina Membranes," *AIChE J.*, **44**(1), 174 (1998).

Xomeritakis, G. and Lin, Y. S., "Fabrication of a Thin Palladium Membrane Supported in a Porous Ceramic Substrate by Chemical Vapor Deposition," *J. Membr. Sci.*, **120**, 261 (1996).